

**MORPHOLOGY CHANGE OF OPTIC NERVE SHEATH (ONS) IN  
IDIOPATHIC INTRACRANIAL HYPERTENSION (IIH) PATIENTS  
(PRE- AND POST-CSF DRAINAGE)**

A Thesis  
Presented to  
The Academic Faculty

by

Chansu Kyle Kim

In Partial Fulfillment of the Requirements for the Degree  
Bachelors of Science in Biomedical Engineering with the Research Option in the  
Wallace H. Coulter Department of Biomedical Engineering

Georgia Institute of Technology  
May 2017

**MORPHOLOGY CHANGE OF OPTIC NERVE SHEATH (ONS) IN  
IDIOPATHIC INTRACRANIAL HYPERTENSION (IIH) PATIENTS  
(PRE- AND POST-CSF DRAINAGE)**

Approved by:

Dr. John N. Oshinski, Associate Professor  
Wallace H.Coulter Department of Biomedical Engineering  
*Georgia Institute of Technology*

---

Signature

---

Date

Dr. S. Balakrishna Pai, Director of Instructional  
Laboratories  
Wallace H. Coulter Department of Biomedical  
Engineering  
*Georgia Institute of Technology*

---

Signature

---

Date

## ACKNOWLEDGEMENTS

The completion of this research could not have been possible without the support and assistance of many people whose names may not all be enumerated. Among all, I would like to express my deep appreciation to the following:

Dr. John N. Oshinski; I really appreciate him for his endless support, kindness, and encouragement ever since I met him in Galway, Ireland. Without his support, I might have not successfully completed my Bachelor's degree. It was pleasure working with him.

Dr. S. Balakrishna Pai; I want to thank him for his kindness, care, and advice throughout the semesters.

I would like to express my gratitude to my lovely family living in South Korea for supporting me until now.

Lastly, I would like to thank my friend, Emily Davis. I am thankful to her for introducing Dr. Oshinski to me, and giving me right advice at the right time which helped me a lot throughout the research term.

# TABLE OF CONTENTS

	Page
1 ACKNOWLEDGEMENTS	3
2 LIST OF FIGURES/SYMBOLS AND ABBREVIATIONS	5-6
3 SUMMARY	7
4 INTRODUCTION	8-9
5 LITERATURE REVIEW	9-11
6 METHODS AND MATERIALS	12-14
SAMPLES	
DATA COLLECTION	
7 RESULTS	14
8 DISCUSSION	14-16
MR IMAGES ACQUISITION	
SELECTING SEEDING POINTS	
DURATIONS	
9 CONCLUSIONS	16
10 FUTURE WORKS	16
11 APPENDIX	17-22
12 REFERENCES	23-24
13 VITA	25

## LIST OF FIGURES

	Page
Figure 1: Vitreoretinal interface is used as reference point.	16
Figure 2: 3-D curved multiplanar reconstruction (MPR) trajectory.	16
Figure 3: Axial images of ON, CSF, and ONS.	17
Figure 4: Dropping Vitreoretinal interface image.	17
Figure 5: Changing intensity of images.	18
Figure 6: Example of selecting seeding point.	18
Figure 7: Calculating CSF area.	19
Figure 8: Examples of dropped images.	19
Figure 9: The average ONSD.	20
Figure 10: The average CSF Area.	20
Figure 11: The CSF Volume.	21
Figure 12: Overgrown ONS contour	21

## **LIST OF SYMBOLS AND ABBREVIATIONS**

CSF	Cerebral Spinal Fluid
IIH	Idiopathic Intracranial Hypertension
ON	Optic Nerve
ONS	Optic Nerve Sheath
ONSD	Optic Nerve Sheath Diameter
MR	Magnetic Resonance
ROI	Regions of Interest

## SUMMARY

Idiopathic Intracranial Hypertension (IIH) is a neurological disorder which can cause the irreversible vision loss due to increased pressure in intracranial space. High pressure in intracranial space expands the optic nerve sheath (ONS), therefore, the optic nerve (ON) gets out of its shape, which triggers the optic nerve twist and globe flattening. Because the elevation of pressure is scientifically unknown, many studies have been conducted to find the root of pressure increase. Meanwhile, none of the previous studies have analyzed the optic nerve sheath diameter (ONSD) change and cerebral spinal fluid (CSF) volume change between pre-CSF drainage vs. post-CSF drainage. This study used T-2 weighted magnetic resonance (MR) imaging techniques to quantitatively measure the ONSD, and compared the ONSD between pre- and post-lumbar puncture procedure. 75% of regions of interest (ROI) which are selected along the optic nerve showed that CSF area and ONSD decreased after the lumbar puncture procedure. Statistical significant difference was found at 11mm anterior to the vitreoretinal interface. In addition, the difference in volume after the lumbar puncture procedure was  $2.7\text{mm}^3$ .

## INTRODUCTION

Idiopathic Intracranial Hypertension (IIH) is a syndrome which is characterized by headache, vomiting and sometimes irreversible vision loss.<sup>1,3</sup> Specifically, abnormal cerebrospinal fluid (CSF) pressure in intracranial space triggers the morphology change in the optic nerve (ON) and the optic nerve sheath (ONS), causing patients to suffer from vision loss as well as other related symptoms. The cause of CSF pressure elevation in intracranial area is clinically and scientifically unknown.<sup>6-8</sup> However, a previous study concluded that humans who were exposed to a different pressure environments had a similar impact on their vision:<sup>1</sup> Astronauts who have been exposed to microgravity tend to have similar symptoms as IIH patients such as posterior globe flattening, ON protrusion, and increased optic nerve diameter (OND) and optic nerve sheath diameter (ONSD).<sup>1</sup> Currently, treatment for IIH is by manually draining cerebrospinal fluid out to reduce the pressure. The diagnosis of IIH can be determined by measuring the pressure in spinal pressure as well as magnetic resonance (MR) imaging. Previous studies indicate that there is a correlation between pressure difference in CSF and ONSD.<sup>4</sup> In Shofty et al's study, regardless of age groups, ONSD increased as CSF pressure increased.<sup>4</sup> ONSD measurement was conducted by looking at examinations of MR images; however, this method does not measure the dimension of the ONS at multiple locations and did not look at changes in ONSD due to CSF drainage.

The purpose of this study is to identify and analyze the diameter change of ONS and ON between pre- and post-CSF drainage by using qualitative and quantitative MR imaging techniques. We believe that this study will further provide quantitative and



qualitative information about whether the appearance including OND and ONSD will return to normal after conducting surgery.

## **LITERATURE REVIEW**

IIH is a disorder that is characterized by elevation of pressure around the brain, and 94% of IIH patients experience headache, 68% have transient visual obscuration, 58% exhibit pulse synchronous tinnitus, and 44% of them suffered from retrobulbar pain.<sup>5</sup> These symptoms are correlated to CSF, which is a clear fluid that is located around the brain which plays a role as a cushion to protect the brain from external damages. Because of high pressure in the CSF, the ONS expands which might induce chronic vision loss (30%).<sup>5</sup> Elevation of pressure in CSF may be caused by pressure difference in patient's surrounding environment; however, IIH patients, who have never exposed to micro-gravity, express similar symptoms as those of astronauts who have been exposed to micro-gravity. This fact undermines the previous assumption that high pressure in CSF is caused solely by environmental factors. Distention of ONS, tortuosity of ON, flattening of the posterior globes and ON head protrusion are the common symptoms for IIH patients.<sup>2</sup> High pressure in CSF can be decreased by placing a flexible tube in the lumbar spine so that CSF can be drained out through a tube, making less fluid in the brain and spine which is known as lumbar puncture procedure or spinal tap. In general, CSF is collected in order to diagnose the diseases or cause of infection<sup>11</sup>. Although treatments for IIH exist, the cause of abnormal pressure in CSF is still unknown.

The MR imaging techniques have been used to confirm the abnormalities in neuro-ophthalmic examination.<sup>1</sup> By using MR imaging technique, previous studies have

been conducted to analyze the degree of symptoms such as ON head protrusion, ON tortuosity and distension of ONS by comparing data between two or more groups.

To analyze the ONSD between healthy and IIH patients, Shofty et al. divided subjects into four age groups: 0-3 years; 3-6 years; 6-12 years; 12-18 years.<sup>4</sup> In order to be consistent with the result, ONSD was measured 1cm anterior to the optic foramina.<sup>4</sup> As a result, the mean of ONSD of healthy groups was significantly smaller than IIH patients group regardless of age and sex.<sup>4</sup>

A previous study examined whether MR imaging findings are associated with visual outcomes in IIH patients. Saindane et al. divided patients into three different groups: no vision loss (n=28), some vision loss (n=10) and severe vision loss (n=8).<sup>3</sup> There was a significant difference in presence of cephaloceles.<sup>3</sup> Therefore, further study was pursued to analyze the differences in demographic and MR imaging findings between IIH patients with cephaloceles and IIH patients without cephaloceles. The degree of pituitary grade was classified from 1 (non-invasive) to 5 (invasive). As a result, the group with severe vision loss had no cephalocels, which was very significant compared to other two groups ( $p=0.01$ ).<sup>3</sup> Therefore, this study stated that it is interesting to hypothesize that the existence of cephalocels and CSF leakage might provide an alternative route to IIH patients: vision loss can be hindered by developing cephalocels, thereby, decreasing the pressure in interstitial fluid.<sup>3</sup> The data shows that young patients are unlikely to have cephalocels and have higher opening pressure (OP) than older patients.<sup>3</sup> Therefore, younger patients have a higher risk of vision loss. This result asserts that age and OP are highly related to the existence of cephalocels and the likelihood of

vision loss.<sup>3</sup> Unfortunately, they could not further perform the study to explore this interesting issue due to a lack of patients.<sup>3</sup>

Most of the previous studies measured ONSD on few ROI by making manual measurements. In our study, edges of the ON and ONS were detected by using region-based image segmentation method, therefore, areas of CSF can be determined by recognition ON and ONS boundaries.<sup>9</sup>

As stated above, no previous studies have evaluated ONSD difference between pre-operation IIH patients group and post-operation IIH patients group. Therefore, our goals include quantitatively measuring the ONSD by using T-2 weighted MR imaging technique to analyze the difference. In addition, we will measure the volumes of CSF by using image processing.

## METHODS AND MATERIALS

### *Samples*

Total number of eight IIH patients underwent a MR imaging examination before the CSF drainage and after the CSF drainage at Emory University Hospital. The median age for the eight patients in this study was 28.875 years (range, 20-42 years). All of the patients were female, and the median weight was 114.515 kg (range, 90.71-136.07 kg). T2-weighted MR imaging was performed with the thickness of 1.5mm. Each patients provided pre- and post- CSF drainage data, and each data contained 29 images.

### *Data Collection*

#### *OsiriX*

OsiriX, an image processing application, was used to select ROIs and to read the digital imaging and communication in medicine (DICOM) file. Vitreoretinal interface, the junction of ON with the globe, was determined as reference point for consistency. In each images, the second ROI was chosen at the point 1.5mm anterior to the vitreoretinal interface as shown on Figure 1. Then, fourteen more ROIs were selected along the ON with the intervals being 1.5mm as shown on Figure 2; therefore, we observed ON from vitreoretinal interface to approximately 3cm anterior to the vitreoretinal interface.

After collecting twenty-nine axial images (Figure 3) along the ON, first image was dropped because image showed the axial image of the vitreoretinal interface (Figure 4). As ROIs approached to the end of the ON, the image resolution gradually decreased. However, some images were very clear at the end of the ON, therefore, no images other than first image were dropped until the entire image acquisitions were completed.

Although ROIs were chosen with 1.5mm intervals, we changed the gap between ROIs to 1mm in order to obtain more data points.

### *MATLAB*

Each image files were renamed in serial order, 000X-00Y, in order to automatically and reproducibly measure the ONSD and CSF area. First four digits with mark “X” represents the patient’s number whereas last three or four digits indicate the ROI. For instance, 0005-0023, indicates that an image is from patient 3 ( $X/2 = 2.5 \rightarrow 3$  rounded up), post-CSF data (X=odd number), and 23mm anterior to the vitreoretinal interface. After all of the images were named in serial order, the intensity of the images were transformed with parameters (low-intensity: 0.05 high-intensity: 0.8) as shown in Figure 5. Next step was to select initial seeding points which takes an important role in CSF contour detection. If the initialization box covers CSF, ON and ONS, CSF contour will be easily detected (Figure 6). In this study, initial seeding points tuned to be (53:85, 75:120), (y-minimum: y-maximum, x-minimum: x-maximum), respectively. This seeding points allowed all of the image data to be tested with no error occurrence. The contour of CSF spreads out from the initialization box until it reaches the preset duration, 200, which displayed the most similar looking image when compared with drawing which is done by hand (Figure 7). After detecting the contour of CSF with 200 iterations, images were transformed to black and white images as shown in figure 7. The area of CSF was measured by transforming image size from pixels to  $\text{mm}^2$ .

### *Data Analysis*

After final data were automatically saved in excel file, we ran the MATLAB code again to consider if data should be either dropped or used. By doing so, such images described in Figure 8 were dropped. In order to obtain large size sample, we combined left and right eyes differentiating between pre- and post-CSF drainage data. For statistical analysis, two tailed unpaired t-test was used to evaluate the statistically significant differences. In order to calculate the volume along the ON, Riemann Sum approximation was used as described below (Figure 11).

$$\text{Volume} = \sum_2^{29} \text{CSF Area (k)} \times 1\text{mm} \text{ (where k is k(mm) anterior to the vitreoretinal interface)}$$

## **RESULTS**

As a result, approximately 75% (21/28 ROIs) showed that the ONSD and CSF area were decreased after the lumbar puncture procedure or post-CSF drainage (Figure 9, 10). The result of average CSF area in pre- and post-CSF are shown in Figure 10. The significant difference was found at 11mm anterior to vitreoretinal interface. The total CSF volume decreased 2.7 mm<sup>3</sup> after the lumbar puncture procedure.

## **DISCUSSION**

The main findings of this study were that CSF area and ONSD decreased after the lumbar puncture procedure, statistically significant difference in CSF area and ONSD were found at appoint where 11mm anterior to vitreoretinal interface. Overall CSF volume decreased

2.7mm<sup>3</sup> after the procedure. This study used the automated edge detection algorithm to find the boundaries whereas previous study manually measured the ONSD. Edge detection method successfully detected the boundaries of ON, CSF, and ONS with clear MR images. However, limitations were found with low quality images.

### *MR Image Acquisition*

The quality of MR images are highly dependent on human natural movement such as breathing, cardiac movement, CSF movement, and blood flow.<sup>10</sup> Mainly, there are two leading causes of MR images artifacts. It can be caused by MR scanner hardware itself or by interaction between hardware and a patient.<sup>10</sup> Some MR images were clear enough to detect the region of CSF with both naked eyes and edge detection algorithm, therefore, image artifacts were not due to hardware itself but interaction between hardware and a patient. Little movement during scanning period diminishes the quality of the images, thereby, more than half of the images were dropped due to low quality.

### *Selecting Seeding Points*

Images were automatically cropped from OsiriX, and axial images were exported to MATLAB file. Because images were exported as DICOM file, no image transitions occurred. Axial images were not displayed in the same pixel due to automatic cropping function in OsiriX. The cropping section was determined by original ROIs selection (red dots) as shown in Figure 2. Although these ROIs were precisely selected, the errors were not avoidable due to manual selection. Therefore, issue arose while selecting perfect seeding points.

### *Duration*

Preset durations, 200, was determined by testing many iterations. 150, 200, and 250 durations were tested to define the adequate durations. The edge detection algorithm was not able to detect the complete edges of ON, CSF and ONS; moreover, detecting edges took a long time with 250 durations, and the contour of CSF overgrew even the edges were already completely detected (Figure 12).

## **CONCLUSION**

It was determined that the ONSD and the CSF area were decreased after undergoing lumbar puncture procedure. Lumbar puncture procedure significantly reduced the CSF area or volume; it did not however significantly reduce the ONSD after the procedure. In addition, the edge detection algorithm successfully detected the boundary of the CSF. However, limitations were found with low quality images.

## **FUTURE WORK**

The abnormal CSF pressure triggered morphology change by inflating ONS. The lumbar puncture procedure reduced the CSF pressure by draining the CSF out from patient's spinal cord. We questioned ourselves that not only ONS but also ON might have affected by elevation in CSF pressure. Therefore, we can observe the ON morphology change to prove whether abnormal CSF pressure significantly affects the characteristic of ON. Because more than half image data were dropped, our next step is to continuously analyze the ONSD with images which has better quality.



## APPENDIX

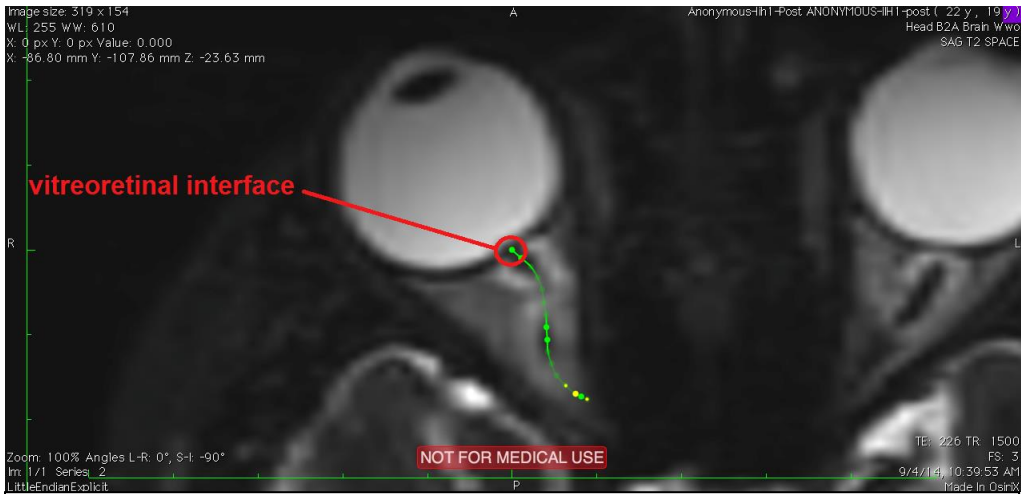


**Figure 1. Vitreoretinal interface is used as reference point.** Vitreoretinal interface (green dot in red circle) was chosen to be reference point for consistency.

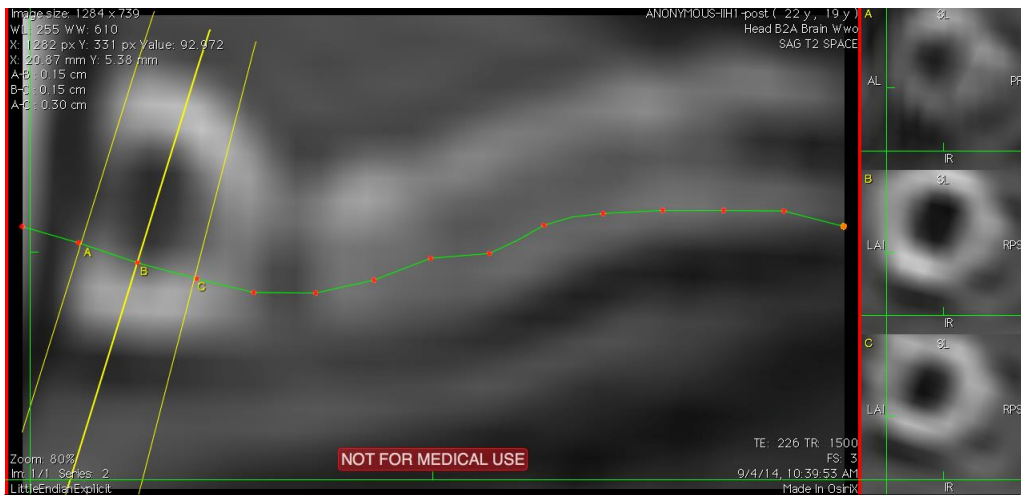


**Figure 2. 3-D curved multiplanar reconstruction (MPR) trajectory.** Red dots represent the ROIs along the ON. A, B, and C are the axial images of ROIs 1.5, 3.0, and 4.5mm posterior to the vitreoretinal interface. Each images are not consistently displayed on same quadrant which could trigger seeding point error.

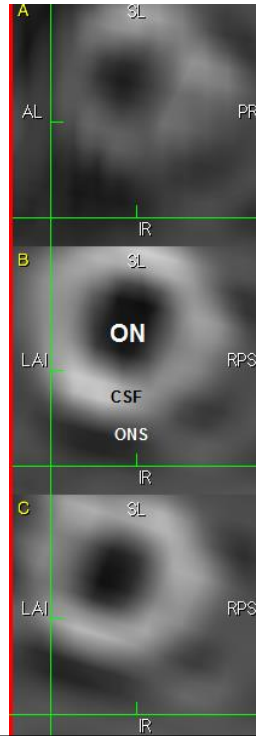


**Figure 3. Axial images of ON, CSF, and ONS.** Doughnut-shaped image on the left includes the ON (inner black circle), CSF (white color), and ONS (outer circle). Image A is an axial image of ON, CSF, and ONS at 1.5mm posterior to the vitreoretinal interface. Image B is an axial image of ON, CSF, and ONS at 3.0mm posterior to the vitreoretinal interface. Image C is an axial image of ON, CSF, and ONS at 4.5mm posterior to the vitreoretinal interface.

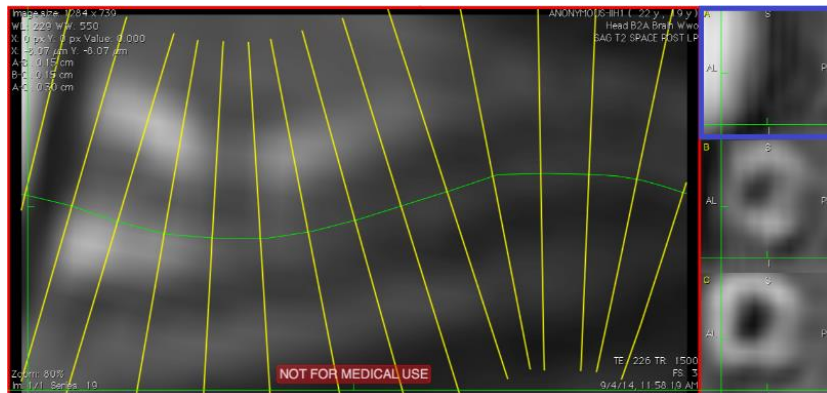


**Figure 4. Dropping Vitreoretinal interface image.** Twenty ROIs were sliced perpendicularly with gaps of 1.5mm. The first ROI (blue box) is the axial image of reference point, vitreoretinal interface, which is going to be dropped from our data.

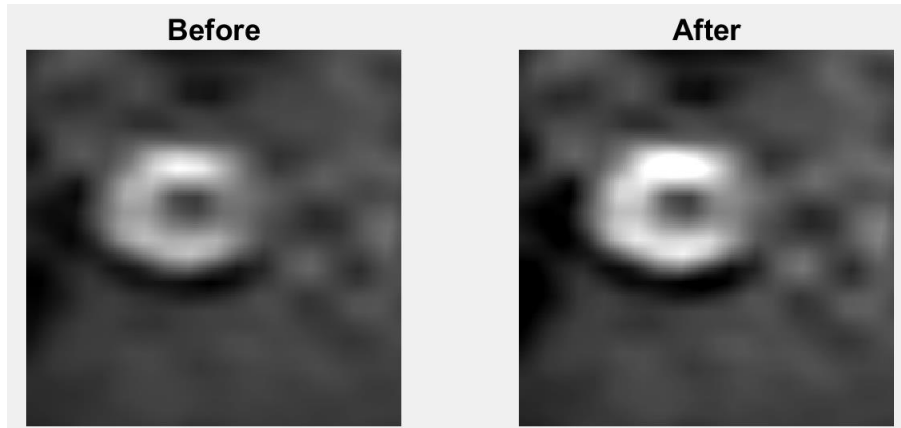
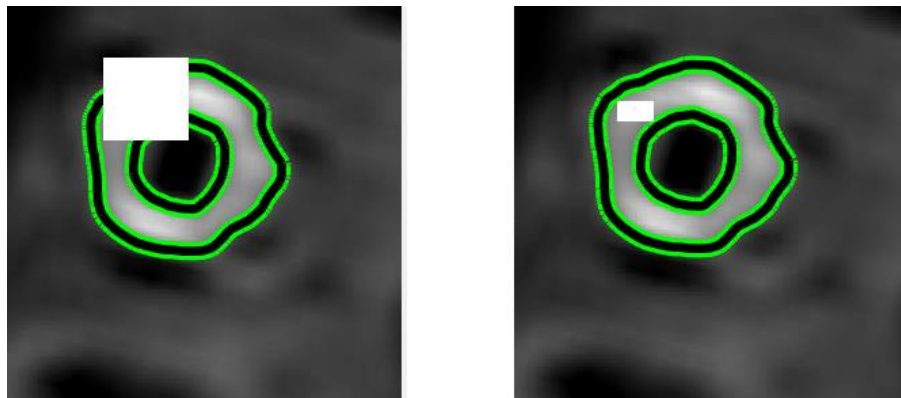


**Figure 5. Changing intensity of images.** Image intensity was changed in order to visualize the CSF better. Parameters were selected after multiple trials:

Low intensity: 0.05

High intensity: 0.8



**GOOD**

**BAD**

**Figure 6. Example of selecting seeding point.** If initialization box (white) is large enough to cover the portion of ONS, CSF, and ON, then detecting CSF contour is available. If not, program will not be able to detect the edge of CSF.

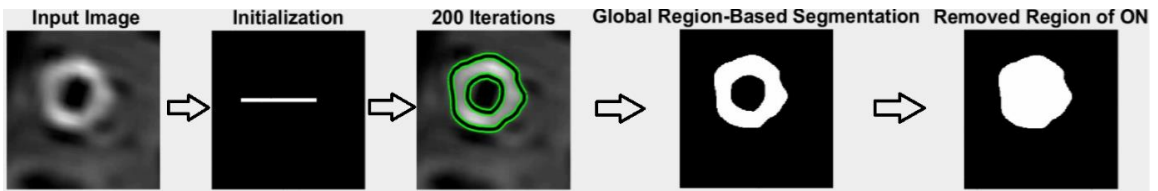


**Figure 7. Calculating CSF area.** After 200 iterations have been done, image is transformed to black and white to easily identify the CSF region (white area on “Global Region-Based Segmentation”) and ONSD. In order to obtain ONSD, we assumed that round white region is a perfect circle show on “Removed Region of ON”.

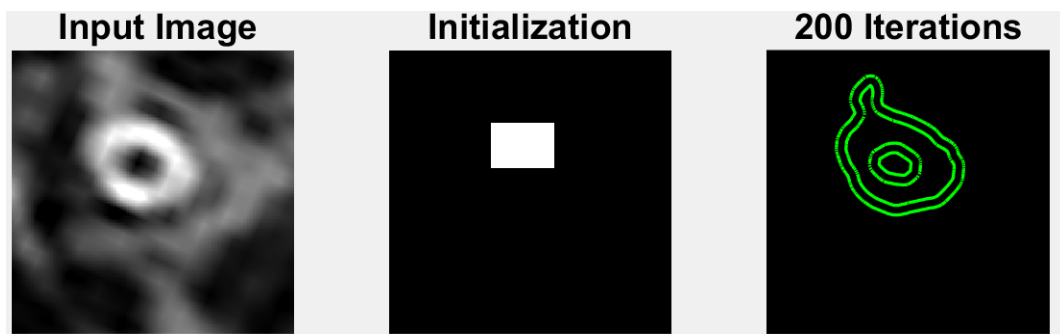


**Figure 8. Examples of dropped images.** Images as shown above (“200 Iterations”) were considered as inappropriate image, thus, they were dropped.

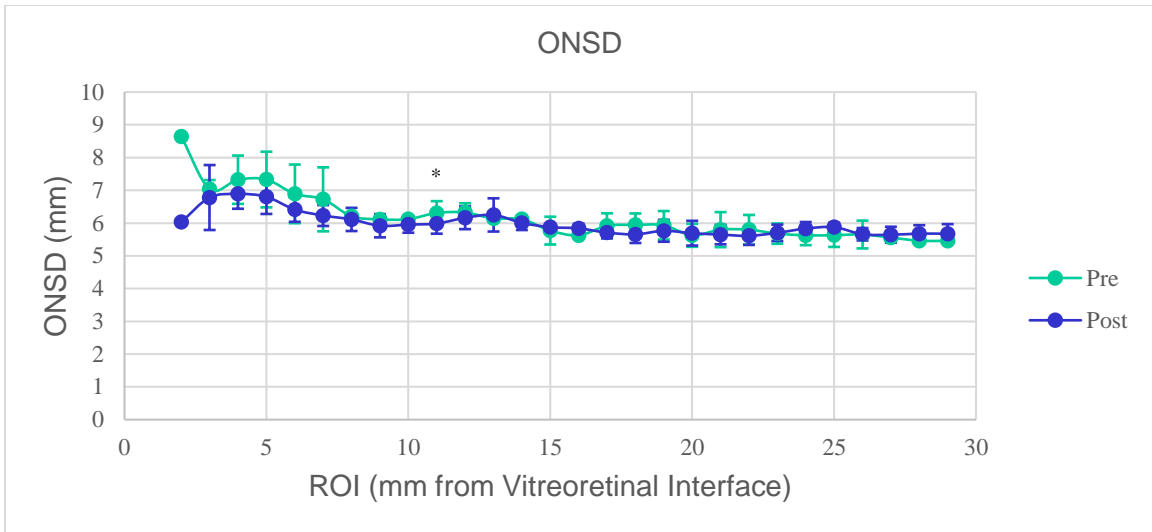


**Figure 9. The average ONSD.** Scatter with smooth line graph was described as shown above. Standard deviations were marked with error bar. Blue line represents the pre-CSF drainage data whereas orange represents the post-CSF drainage data. The statistical significant difference was found at a point 11mm anterior to vitreoretinal interface (\*).

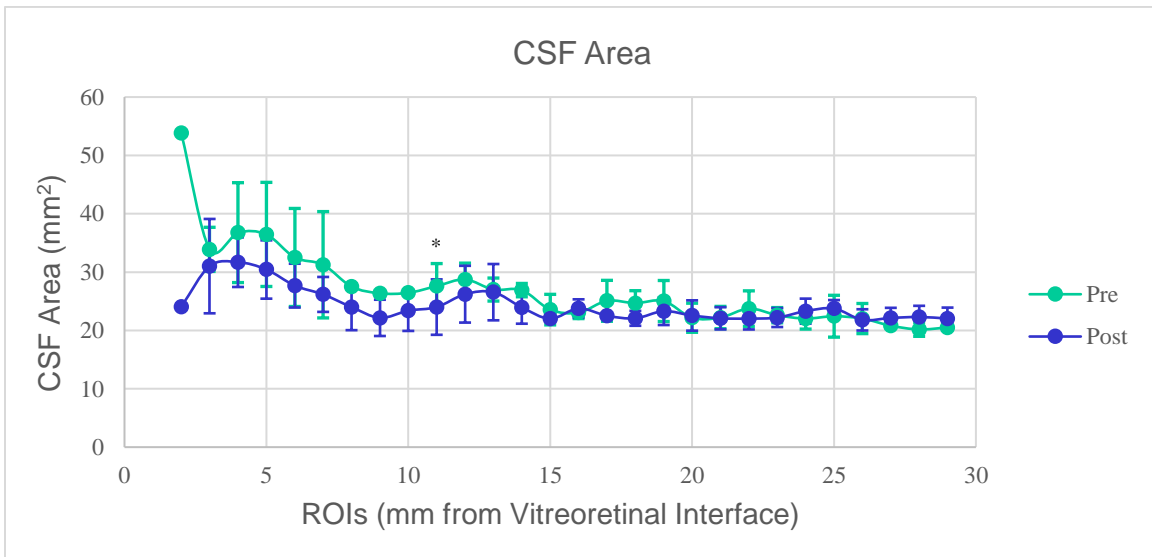


**Figure 10. The average CSF Area.** Scatter with smooth line graph was described as shown above. Standard deviations were marked with error bar. Blue line represents the pre-CSF drainage data whereas orange represents the post-CSF drainage data. The statistical significant difference was found at a point 11mm anterior to vitreoretinal interface (\*).



**Figure 11. The CSF Volume.** The CSF volume along the ON was calculated by following equation:

$$\text{Volume} = \sum_{k=2}^{29} \text{CSF Area (k)} \times 1\text{mm} \text{ (where k is k(mm) anterior to the vitreoretinal interface)}$$

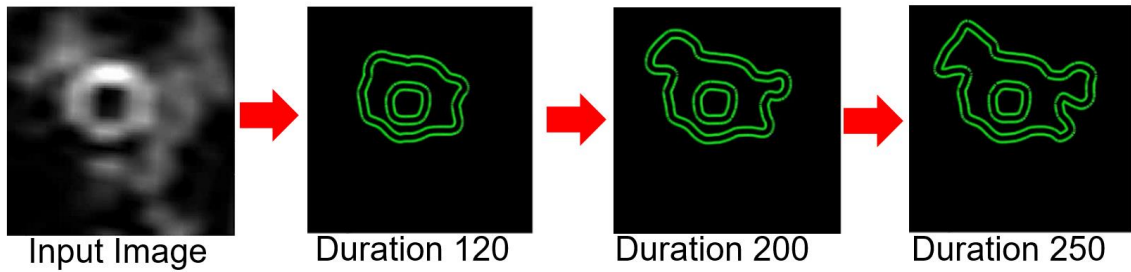


**Figure 12. Overgrown ONS contour.** The edge detection algorithm was keep detecting the edges even the contour was already close enough to input image at “duration 120”.

## REFERENCES

- [1] Kramer, L. A., Sargsyan, A. E., Hasan, K. M., Polk, J. D., & Hamilton, D. R. (2012). Orbital and Intracranial effects of Microgravity: Findings at 3-T MR imaging. *Radiology*, 263(3), 819–827. doi:10.1148/radiol.12111986
- [2] Roberts, D. R., Zhu, X., Tabesh, A., Duffy, E. W., Ramsey, D. A., & Brown, T. R. (2015). Structural brain changes following long-term 6 head-down tilt bed rest as an analog for Spaceflight. *American Journal of Neuroradiology*, 36(11), 2048–2054. doi:10.3174/ajnr.a4406
- [3] Saindane, A. M., Bruce, B. B., Riggeal, B. D., Newman, N. J., & Biousse, V. (2013). Association of MRI findings and visual outcome in Idiopathic Intracranial hypertension. *American Journal of Roentgenology*, 201(2), 412–418. doi:10.2214/ajr.12.9638
- [4] Shofty, B., Ben-Sira, L., Constantini, S., Freedman, S., & Kesler, A. (2011). Optic nerve sheath diameter on MR imaging: Establishment of norms and comparison of pediatric patients with Idiopathic Intracranial hypertension with healthy controls. *American Journal of Neuroradiology*, 33(2), 366–369. doi:10.3174/ajnr.a2779
- [5] Wall, M. (2013). Idiopathic Intracranial Hypertension and the Idiopathic Intracranial Hypertension Treatment Trial. *Journal of Neuro-Ophthalmology*, 33(1), 1-3. doi:10.1097/wno.0b013e3182819aee
- [6] Kesler, A., Goldhammer, Y., & Gadoth, N. (2001). Do Men With Pseudotumor Cerebri Share the Same Characteristics as Women? A Retrospective Review of 141 Cases. *Journal of Neuro-ophthalmology*, 21(1), 15-17. doi:10.1097/00041327-200103000-00004
- [7] Radhakrishnan, K. (1993). Idiopathic Intracranial Hypertension (Pseudotumor Cerebri). *Archives of Neurology*, 50(1), 78. doi:10.1001/archneur.1993.00540010072020
- [8] Ahlskog JE, O'Neill BP. Pseudotumor cerebri. *Ann Intern Med* 1982;97:249-56

- [9] Mathworks. (2008). Active Contour Segmentation (R2015b). Retrieved March 31, 2016 from [https://www.mathworks.com/matlabcentral/fileexchange/19567-active-contour-segmentation/content/regionbased\\_seg/region\\_seg\\_demo.m](https://www.mathworks.com/matlabcentral/fileexchange/19567-active-contour-segmentation/content/regionbased_seg/region_seg_demo.m)
- [10] Krupa, K., & Bekiesińska-Figatowska, M. (2015). Artifacts in Magnetic Resonance Imaging. *Polish Journal of Radiology*, 80, 93–106.  
<http://doi.org/10.12659/PJR.892628>
- [11] Lumbar Puncture. (n.d.). Retrieved April 14, 2017, from <http://www.webmd.com/brain/lumbar-puncture#1>



## **VITA**

### **CHANSU KYLE KIM**

Kim was born in Seoul, South Korea. He attended College in Chanute, Kansas, received an Associate of Science degree at Neosho County Community College in 2012 and a B.S in Biomedical Engineering at Georgia Institute of Technology in 2017. He spent 21 months in the Republic of Korean Army as a Sergeant (E-5) and Squad Commander in 2013. Kim's interests are medical devices, robotics and designing medical products.